Diurnal temperature range variation and its causes in a semiarid region from 1957 to 2006

Article *in* International Journal of Climatology · February 2014

DOI: 10.1002/joc.3690

4 authors:

Fuxing Wang
Le Laboratoire de Météorologie Dynamique (…
7 PUBLICATIONS **88** CITATIONS
SEE PROFILE

Chi Zhang
Dalian University of Technology
49 PUBLICATIONS **398** CITATIONS
SEE PROFILE

Yong Peng
Dalian University of Technology
43 PUBLICATIONS **300** CITATIONS
SEE PROFILE

Huicheng Zhou
Dalian University of Technology
88 PUBLICATIONS **536** CITATIONS
SEE PROFILE

INTERNATIONAL JOURNAL OF CLIMATOLOGY
Int. J. Climatol. **34**: 343–354 (2014)
Published online 12 March 2013 in Wiley Online Library
(wileyonlinelibrary.com) DOI: 10.1002/joc.3690

RMetS
Royal Meteorological Society

Diurnal temperature range variation and its causes in a semiarid region from 1957 to 2006

Fuxing Wang,[ab]* Chi Zhang,[a] Yong Peng[a] and Huicheng Zhou[a]

[a] *Institute of Water Resources and Flood Control, Dalian University of Technology, Dalian 116024, China*
[b] *Laboratoire de Météorologie Dynamique du CNRS, 4 Place Jussieu, case courrier 99, 75252 Paris Cedex 05, France*

ABSTRACT: The diurnal temperature range (DTR) is an important indicator of climate change, and it has decreased worldwide since the 1950s, particularly over arid and semiarid regions. This study analyses the effect of meteorological and anthropogenic factors on DTR variation to investigate the possible causes of DTR decreases in semiarid climates. The study region is located in northeast China, and the study period is from 1957 to 2006. There are three main results. First, the rate of decrease in the DTR is −1.24 K per 50 years. This decrease is mainly attributed to the increasing daily minimum temperature rate (T_{min}, 2.24 K per 50 years), which is greater than the change in the daily maximum temperature (T_{max}, 1.00 K per 50 years). Second, sunshine duration (SD) appears to be the most significant meteorological factor that determines the DTR through downward shortwave radiation ($R_{sw,d}$) and surface soil moisture (SM). The effect of $R_{sw,d}$ is larger for T_{max} than for T_{min}; therefore, the decrease in $R_{sw,d}$ results in a smaller increase in T_{max} than in T_{min}. On the other hand, the increase in SM can strengthen daytime latent heat release, and the increase in T_{max} is then slowed because of the cooling effect of evaporation. The precipitation values and the leaf area index show a negative correlation with the DTR, whereas the cloud amount and the relative humidity appear not to be main causes of the DTR decrease in this region. Finally, atmospheric aerosols can reduce the SD by 0.27 h year^{-1} by decreasing atmospheric transparency, as indicated by an analysis of the Total Ozone Mapping Spectrometer Aerosol Index from 1979 to 2005. The decrease in direct solar radiation is the main cause of decreases in $R_{sw,d}$. These findings will provide references for DTR variation studies in similar climates.

KEY WORDS diurnal temperature range; climate variation; causes; semiarid region; long-term

Received 12 January 2012; Revised 24 January 2013; Accepted 11 February 2013

1. Introduction

The diurnal temperature range (DTR) is considered as a suitable measure of climate change because of its sensitivity to variations in the radiative energy balance (Dai *et al.*, 1999; Przybylak, 2000; Sun *et al.*, 2006; Makowski *et al.*, 2008). The DTR has decreased worldwide since the 1950s, mainly as a result of asymmetric diurnal changes in the daily temperature maximums (T_{max}) and minimums (T_{min}) (Karl *et al.*, 1991; Karl *et al.*, 1993; Dai *et al.*, 1997; Easterling *et al.*, 1997; Dai *et al.*, 1999; Stone and Weaver, 2002; IPCC, 2007; Zhou *et al.*, 2008; Zhou *et al.*, 2009; Lai and Cheng, 2010; Fan *et al.*, 2011). The warming trend for T_{min} is usually stronger than for T_{max}. In some regions, the T_{min} has increased, but the daytime T_{max} has decreased (Karl *et al.*, 1991; Karl *et al.*, 1993; Türkes *et al.*, 1996; Dai *et al.*, 1997; Easterling *et al.*, 1997; Dai *et al.*, 1999; Liu *et al.*, 2004b).

Many studies have determined that the reduction in DTR is a consequence of increases in cloud cover, soil moisture (SM) and precipitation (Karl *et al.*, 1993; Dai *et al.*, 1997; Dai *et al.*, 1999; Stone and Weaver, 2002). Clouds have a negative effect on DTR by reflecting sunlight during the day (decrease T_{max}) and enhancing downward longwave radiation ($R_{lw,d}$) at night (increase in T_{min}) (Dai *et al.*, 1997; Dai *et al.*, 1999; Zhou *et al.*, 2009). SM may reduce the DTR via a surface evaporative cooling effect on T_{max}, and precipitation may affect DTR indirectly by increasing SM content (Dai *et al.*, 1997, 1999). Zhou *et al.* (2009) found that a decline in DTR is generally correlated with a decrease in the leaf area index (LAI), which is determined by climate conditions (e.g. precipitation). Some studies have found that land cover changes can reduce the DTR through the modification of land surface properties (e.g. emissivity) over some regions (Feddema *et al.*, 2005; Zhou *et al.*, 2007). Other factors, such as atmospheric aerosols and greenhouse gases, may also contribute to the decrease in DTR (Stone and Weaver, 2002; Liu *et al.*, 2004b; IPCC, 2007; Zhou *et al.*, 2007). Aerosols may affect the DTR by reflecting solar radiation and by modifying cloud properties, whereas greenhouse gases may play a role in altering the DTR by controlling the surface energy and hydrological balance (Zhou *et al.*, 2007; Zhou *et al.*, 2009).

Although various studies on DTR variation have been conducted, the investigation of DTR change mechanisms

* Correspondence to: F. Wang, Laboratoire de Météorologie Dynamique du CNRS, 4 Place Jussieu, case courrier 99, 75252 Paris Cedex 05, France. E-mail: wangfuxings@gmail.com

is still necessary because of the complexity of the climatology (Dai *et al.*, 1997; Dai *et al.*, 1999; Sun *et al.*, 2006; Martínez *et al.*, 2010). It is difficult to explain DTR changes explicitly based on one parameter alone (Easterling *et al.*, 1997). DTR variation has regional characteristics because of the various changes in local climate due to the complicated interactions of local climate and other anthropogenic factors (Karl *et al.*, 1991; Karl *et al.*, 1993; Easterling *et al.*, 1997; Liu *et al.*, 2004b). In fact, the largest decreases in DTR were observed mostly over arid or semiarid regions (e.g. North China and western African Sahel) where drought has occurred (Zhou *et al.*, 2007).

In this study, the effects of climate elements [e.g. precipitation, sunshine duration (SD), pan evaporation (PE), surface SM, relative humidity (RH), solar radiation and cloud cover], vegetation indicators (LAI) and anthropogenic factors (aerosols) on DTR change are examined using 50 years (1957 to 2006) of daily observation data over the upper Second Songhua River basin (USSR). The USSR borders northeast China, and it is characterized by a temperate, semiarid continental climate; the annual mean precipitation is approximately 700 mm (Wang *et al.*, 2011; Wang *et al.*, 2012). The aim of this work is to investigate the possible causes of DTR variation and the mechanisms behind such variation in a semiarid climate. This work is unique in that the comprehensive observations (including climatology, vegetation and aerosols) are analysed within a semiarid region. The results of this study will provide references for DTR variation studies as well as for regional climate modelling.

In this paper, Section 2 describes datasets and analytical methods. Section 3 presents the results and discussions, which include temperature variation analyses, the possible causes of DTR changes and the role of aerosols in SD changes. Conclusions and future directions are provided in Section 4.

2. Data and methodology

2.1. Data

2.1.1. In situ observations

The ground-based meteorological daily observations include T_{max}, T_{min}, average temperature (T_m), cloud amount (CA), mean surface RH and SD. The data were obtained from the China Meteorological Administration (CMA) National Meteorological Information Center (NMIC) through its website, http://cdc.cma.gov.cn/. The daily precipitation data were provided by Songliao Water Resources, Ministry of Water Resources (SWR MWR). The data from 6 meteorological sites and 15 rain gauges were collected (Figure 1(b)). The available data cover the period from 1957 to 2006 (Table 1). The simple linear interpolation method and the stepwise regression method were used to fill in missing data gaps when gaps are up to 7 days in length and more than 7 days in length, respectively (Liu *et al.*, 2004b).

Table 1. The data for the USSR.

Variable	Station/resolution	Period
Precipitation	15 rain gauges	1957–2006
Meteorology[a]	6 stations	1957–2006
Solar radiation	3 stations	1961–2006
Surface 10-cm SM	2 stations	1993–2006
PE	1 station	1981–2006
AVHRR LAI	16 km × 16 km	July 1981–May 2001
TOMS aerosol index	1.25° × 1°	1979–1992, 1997–2005

[a]The meteorology data include daily maximum, minimum and mean temperature, and daily RH, CA and SD.

The daily downward shortwave radiation ($R_{sw,d}$) data were collected from the CMA at the Changchun, Shenyang and Yanji stations (Figure 1(b)). The data period from 1961 to 2006 was selected because the observations for all three stations were available (Table 1). Yanishevsky thermoelectric pyranometers were used to measure surface solar radiation data collected before 1993, whereas DFY-4 pyranometers were used for data collected after 1993. It has been reported that the uncertainty of the measurements is <5% (Shi *et al.*, 2008). All of the above meteorological data were then interpolated to 1000-m cells through inverse-distance weighting to calculate the basin average value and the spatial distributions.

The daily PE was observed using a E601-type evaporation pan at the Wudaogou station (Figure 1(b)) from 1981 to 2006 (Table 1). The data were obtained from SWR MWR. The surface SM observations from the Huadian and Yangzishao stations (Figure 1(b)) were provided by the CMA NMIC. SM was measured every 10 days (i.e. on the 8th, 18th and 28th of every month) in the warm season (May–September) from 1992 to 2008 using the gravimetric technique (Wang and Zeng, 2011). The values for the top 10 cm (mass percentage) from 1993 to 2006 are used here.

2.1.2. Satellite observations

The dynamic vegetation parameter LAI is generally defined as one-sided green leaf area per unit ground surface area (Myneni *et al.*, 1997). The LAI data were obtained from the Advanced Very High Resolution Radiometer (AVHRR) 16-km monthly product (Myneni *et al.*, 1997) through ftp://primavera.bu.edu/pub/datasets. The data are available from July 1981 to May 2001.

The Total Ozone Mapping Spectrometer (TOMS) Aerosol Index (AI) data were obtained from the NASA Goddard Earth Sciences Data Information Services Center (GES DISC, http://acdisc.gsfc.nasa.gov/). AI is a qualitative measure of the presence of UV absorbing aerosols, such as mineral dust and smoke (Herman *et al.*, 1997). The positive AI values and the negative AI values are associated with absorbing (mineral dust, smoke and volcanic aerosols) and non-absorbing (sulphate and sea salt particles) aerosols, respectively (Torres *et al.*, 1998; Torres *et al.* 2002). Near-zero values indicate cloud presence. The daily TOMS/AI data utilized in the research are the version 8 data, which have a spatial resolution

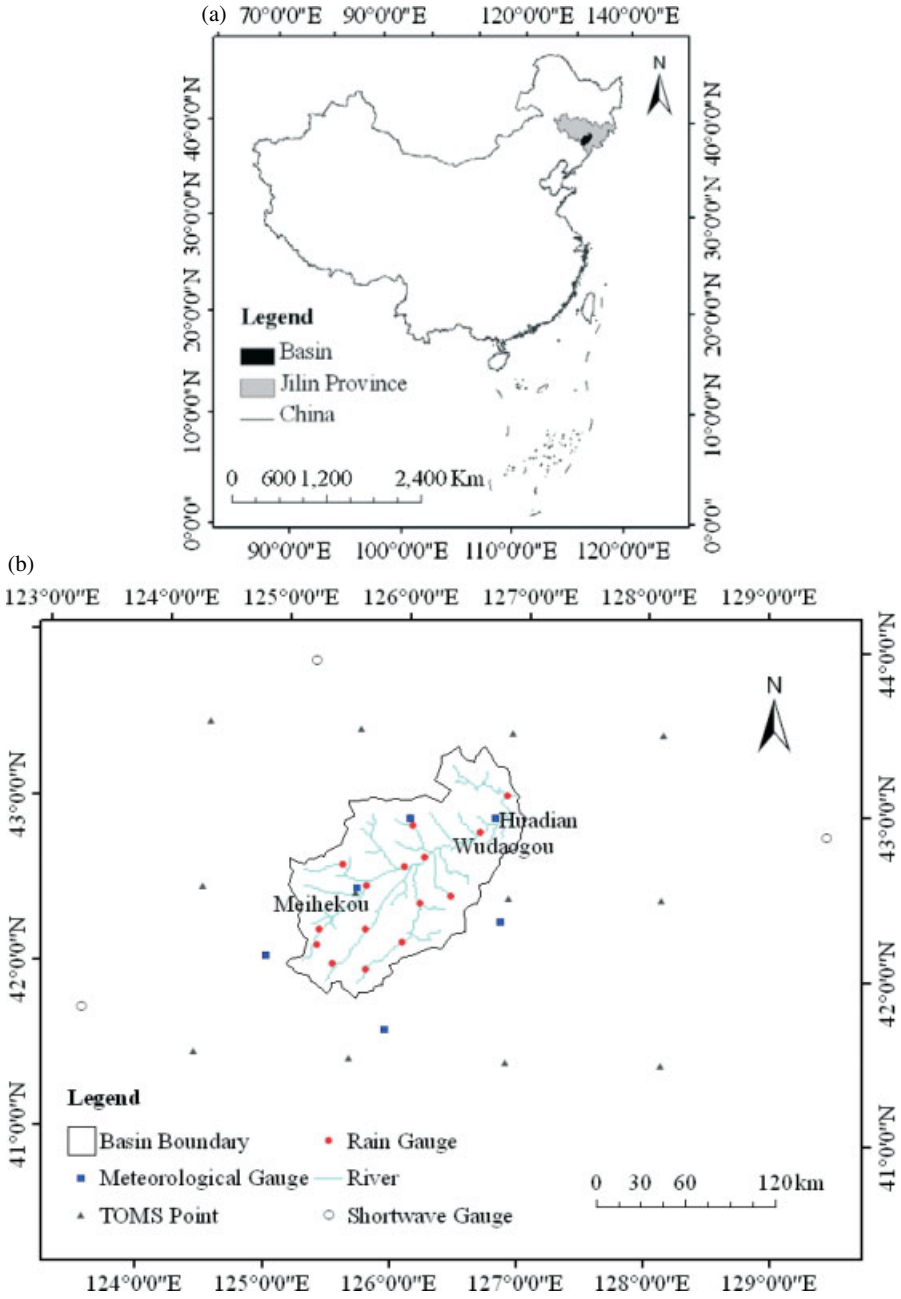

Figure 1. The USSR: (a) the location within China and (b) the dataset.

of $1.25^\circ \times 1^\circ$ with global coverage. For the period from 1979 to 1992, we used daily TOMS Nimbus-7 data, and for the period from 1997 to 2005, we used TOMS Earth Probe data.

2.2. Methods

2.2.1. Trend magnitude calculation

A linear regression model (Tang *et al.*, 2007, 2008) is used to calculate the trend magnitude. The regression function is

$$y = \beta \times t + \gamma \tag{1}$$

where t is the time number and y is the data value at time t; the regression weight β and noise term γ are calculated according to Equations (2) and (3)

$$\beta = \frac{\left(n\sum_{i=1}^{n} t_i y_i - \sum_{i=1}^{n} t_i \sum_{i=1}^{n} y_i\right)}{\left[n\sum_{i=1}^{n} t_i^2 - \left(\sum_{i=1}^{n} t_i\right)^2\right]} \tag{2}$$

$$\gamma = \frac{\sum_{i=1}^{n} y_i - \beta \sum_{i=1}^{n} t_i}{n} \tag{3}$$

where n is the time-series number. Student's t-test is applied to evaluate the statistical significance of the

trends. The significance of a correlation coefficient r is tested with

$$t_s = \frac{r}{\sqrt{\left(1 - r^2\right) / (n - 2)}} \tag{4}$$

where the distribution of t_s is approximately that of the t-distribution with $n - 2$ degrees of freedom. The trend magnitude ΔY and relative trend magnitude $\Delta Y'$ during the study period are estimated using Equations (5) and (6) if a trend is detected:

$$\Delta Y = \beta \times n \tag{5}$$

$$\Delta Y' = \frac{100 \times n \times \Delta Y}{\sum_{i=1}^{n} y_i} \tag{6}$$

The linear trend is removed from the forcing data to compare the observed trends with non-change scenarios.

$$y\_rm = y_i - (\beta \times t_i + \gamma) + \overline{y} \tag{7}$$

where y_rm is the time series data after removing tendency and $\overline{y}$ is the mean value of the nonlinear trend time series. The $\overline{y}$ value is set to the mean value of the first 10 years of data (1957–1966).

2.2.2. *Variable normalization*

The normalized variable (X_{norm}) is used to compare the variables with different scales. X_{norm} is calculated using Equations (8) and (9):

$$X_{norm} = \frac{\left(X_{oi} - \overline{X}_o\right)}{\sigma} \tag{8}$$

$$\sigma = \sqrt{\frac{\left(\sum_{i=1}^{n} \left(X_{oi} - \overline{X}_o\right)^2\right)}{n}} \tag{9}$$

where X_{oi} is the observed value, $\overline{X}_o$ is the mean value of X_{oi} over the comparison period, n is the total number of time series for comparison, and σ is the standard deviation.

3. Results and discussions

3.1. Temperature variation analysis

3.1.1. *Temporal analysis*

Figure 2(a)–(d) show the variations in the annual means for the T_{max}, T_{min}, T_m and DTR over the USSR from 1957 to 2006. In general, the t-test is significant for all four of these variables (Table 2).

The T_{max} increases at a rate of 1.00 K per 50 years (Figure 2(a)). This trend is higher than that reported for China as a whole (0.635 K per 50 years) between 1955 and 2000 (Liu *et al.*, 2004b) and for the Northern Hemisphere (0.435 K per 50 years) between 1950 and 1993 (Easterling *et al.*, 1997). Figure 2(b) shows that the T_{min} increases at a rate of 2.24 K per 50 years from 1957 to 2006. This trend is also higher than previous analyses for China (1.615 K per 50 years) between 1957 and 2006 (Liu *et al.*, 2004b) and for the Northern Hemisphere (0.92 K per 50 years) between 1950 and 1993 (Easterling *et al.*, 1997). For T_m (Figure 2(c)), we calculate a rate of change equal to 1.68K per 50 years between 1957 and 2006, whereas Liu *et al.* (2004b) reported a value of 0.59 K per 50 years from 1955 to 1990. For the entire study period, we calculate the rate of change in DTR as −1.24 K per 50 years (Figure 2(d)). This is higher than the rate of −1.01 K per 50 years reported in a previous study on China (Liu *et al.*, 2004b) and of 0.445 K per 50 years for the Northern Hemisphere (Easterling *et al.*, 1997). As previous studies noted, the decreasing trend in DTR is mainly the result of T_{min} increasing at a rate outpacing increases in T_{max} (e.g. Dai *et al.*, 1997; Easterling *et al.*, 1997; Dai *et al.*, 1999; Liu *et al.*, 2004b). This result further supports the previous conclusions.

Table 2. The change in climate and vegetation conditions in the USSR.

Variable	Averaged	Trend[a] (per 50 years)	Relative trend (%)	t-test
T_{max} (K)	284.76	1.00	0.35	**3.07**
T_{min} (K)	272.16	2.24	0.82	**7.84**
T_m (K)	278.01	1.68	0.61	**6.06**
DTR (K)	12.60	−1.24	−9.86	**5.41**
CA	0.49	−0.09	−19.29	**7.96**
P (mm year^{-1})	715.46	2.55	0.36	0.04
RH	0.70	−0.02	−3.11	**3.23**
SD (h)	6.54	−0.72	−11.05	**4.70**
$R_{sw,d}$ (W m^{-2})	154.69	−12.03	−7.78	**3.62**
PE (mm)	491.99	31.84	6.47	0.87
SM_HD (%)	86.62	0.20	0.23	0.03
SM_MHK (%)	81.69	1.22	1.49	0.22
LAI	2.71	0.03	1.08	0.33

The bold values indicate that the t-test is significant. [a]A significance level of 5% is used to detect the trend.

3.1.2. *Spatial analysis*

Figure 3 depicts the spatial distribution of the annual mean values for the T_{max}, T_{min}, T_m and DTR trend magnitudes over the USSR from 1957 to 2006. The warming trends appear in all parts of the region. The greatest increase in T_{max} is found in the southeastern part of the region, and the rate slows as we move from the southeast to the northwest (Figure 3(a)). The T_{min} (Figure 3(b)) and the T_m (Figure 3(c)) show similar spatial distributions of trend magnitude. The largest increasing trend is found in the southeastern part of the region, and the smallest value is found in the northwestern part of the basin. The trend gradually decreases from southeast to northwest. The spatial distribution of the DTR (Figure 3(d)) shows variation trends that are opposite to those of T_{min} and T_m. This is reasonable because the decrease in DTR is mainly caused by the greater rate of increase in T_{min} relative to T_{max}.

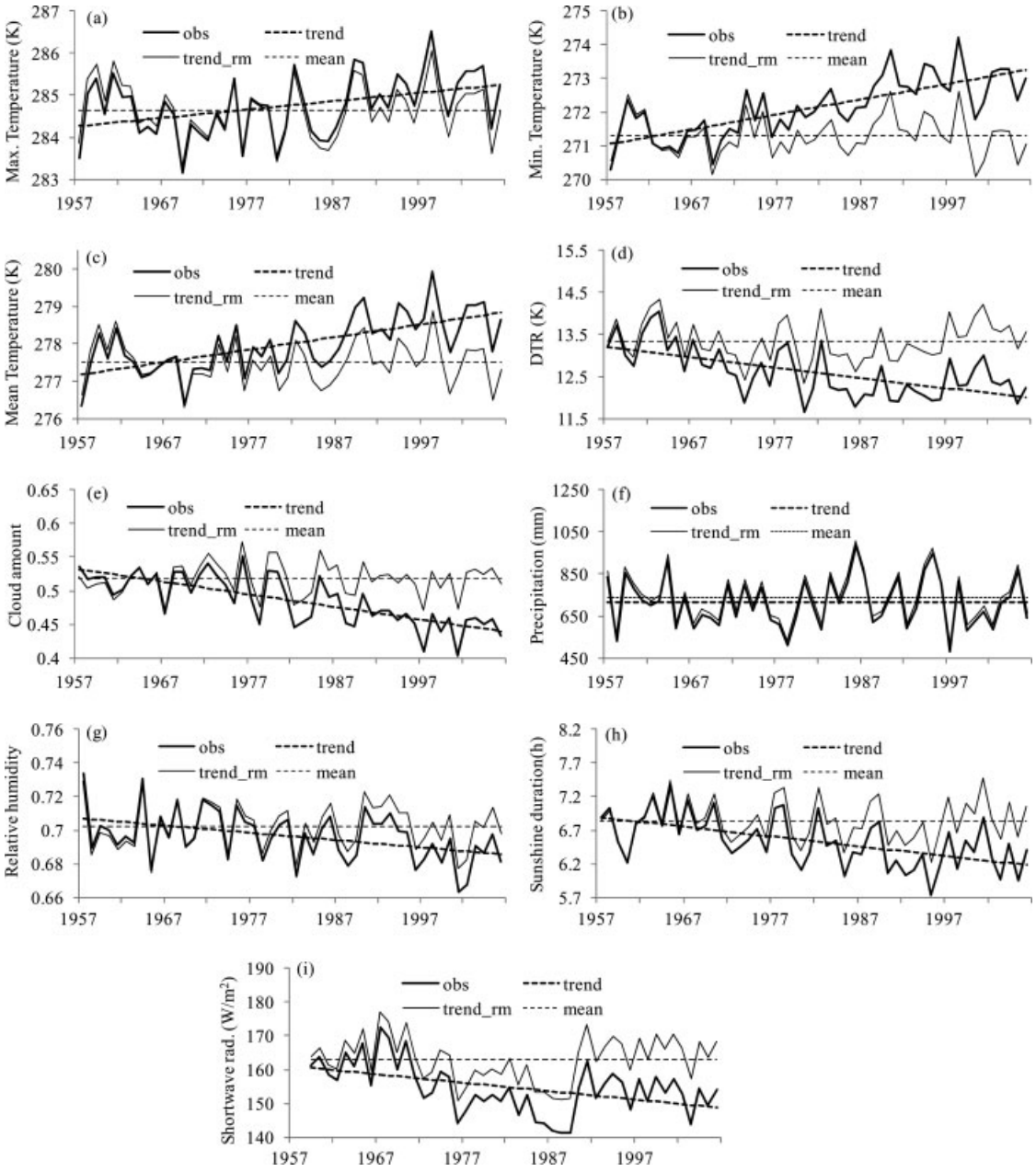

Figure 2. The changes of maximum temperature (a), minimum temperature (b), mean temperature (c), DTR (d), CA (e), precipitation (f), RH (g), SD (h) and downward shortwave radiation (i) with (bold line) and without linear tendency (thin line) in the USSR from 1957 to 2006. The solar radiation data is from 1959 to 2006. The mean value (dashed thin line) is obtained by averaging the observations from the first 10 years (1957–1966 or 1961–1970).

3.1.3. Summary

From 1957 to 2006 over the USSR, the T_m, T_{max}, and T_{min} increase, whereas the DTR decreases. All four variables (T_m, T_{max}, T_{min} and DTR) change at a rate higher than that reported for China as a whole and for the Northern Hemisphere. It should be noted that the USSR is characterized by a semiarid continental climate. As Zhou *et al.* (2007) noted, the greatest decreases in the DTR were observed mostly over arid or semiarid regions (e.g. North China). Changes in the DTR can result from a number of complicated mechanisms. Because DTR is an important indicator of climate variation, the causes of the DTR variation in this semiarid environment are investigated in the following section.

3.2. The possible causes of DTR decrease

In this section, the causes of DTR variation are investigated by analysing the temporal trend and the correlation between the DTR and climatological factors. These factors include CA, precipitation, RH, SD, $R_{sw,d}$, PE, top 10-cm surface SM and LAI.

3.2.1. Trend analysis

Figure 2(e)–(i) illustrate the variation in mean annual CA, precipitation, RH, SD and $R_{sw,d}$ over the USSR

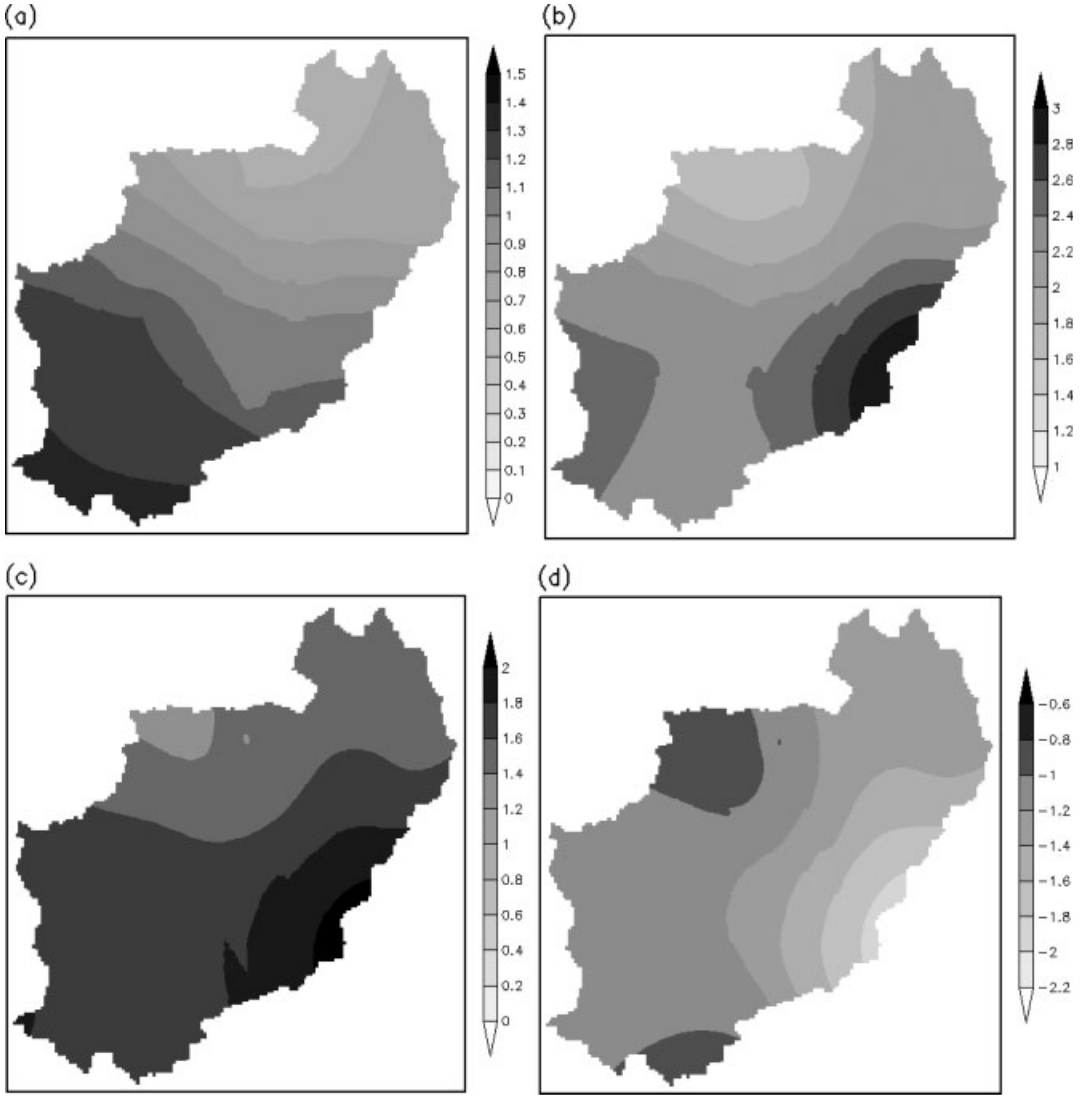

Figure 3. The spatial distribution of temperature changes in the USSR from 1957 to 2006: maximum temperature (a), minimum temperature (b), mean temperature (c) and the DTR (d) trend.

from 1957 to 2006. Figure 4 depicts the change in the mean annual PE at the Wudaogou station (Figure 1(b)), SM at the Huadian (SM_HD) station and the Meihekou (SM_MHK) station, and LAI. In general, the t-test for CA, RH, SD, and $R_{sw,d}$ is significant, whereas it is not significant for other variables (Table 2).

Figure 2(e) shows the change of CA from 1957 to 2006. The CA decreases at a rate of 0.09 per 50 years between 1957 and 2006. This decreasing trend is consistent with the value of 0.05–0.15 per 50 years for northern China between 1954 and 2001 (Qian *et al.*, 2006), whereas it is slightly lower than the value of 0.10–0.15 per 50 years for northeast China between 1954 and 1994, as reported by Kaiser (2000). Many studies (e.g. Campbell and Vonder Haar, 1997; Dai *et al.*, 1997; Dai *et al.*, 1999; Liu *et al.*, 2004b) noted that cloud cover has a negative effect on DTR. During the day, clouds can decrease T_{max} by reducing incident shortwave solar radiation, and they can increase T_{min} by intercepting outgoing longwave radiation at night (Campbell and Vonder Haar, 1997; Liu *et al.*, 2004b). Decreasing CA would increase the DTR during this time period, but the observed DTR shows a decreasing trend. This result indicates that the cloud cover change is not the major cause of the DTR variation in this region.

Figure 2(f) plots precipitation trends from 1957 to 2006. A slight increasing trend was detected in this region, but the variation is not significant (Table 2). Previous studies have shown that precipitation is negatively correlated with DTR through surface evaporation cooling (Dai *et al.*, 1999).

Figure 2(g) gives the variation of RH from 1957 to 2006. The RH decreases at a rate of −0.02 per 50 years from 1957 to 2006. The water vapour reduces the DTR by absorbing solar radiation (Dai *et al.*, 1999; Liu *et al.*, 2004b). In this region, the variation trends for RH and the DTR are the same. It is then concluded that the dampening effect of RH is limited in this region.

Figure 2(h) depicts the annual SD variation from 1957 to 2006. The SD decreases at a rate of 0.72 h per 50 years

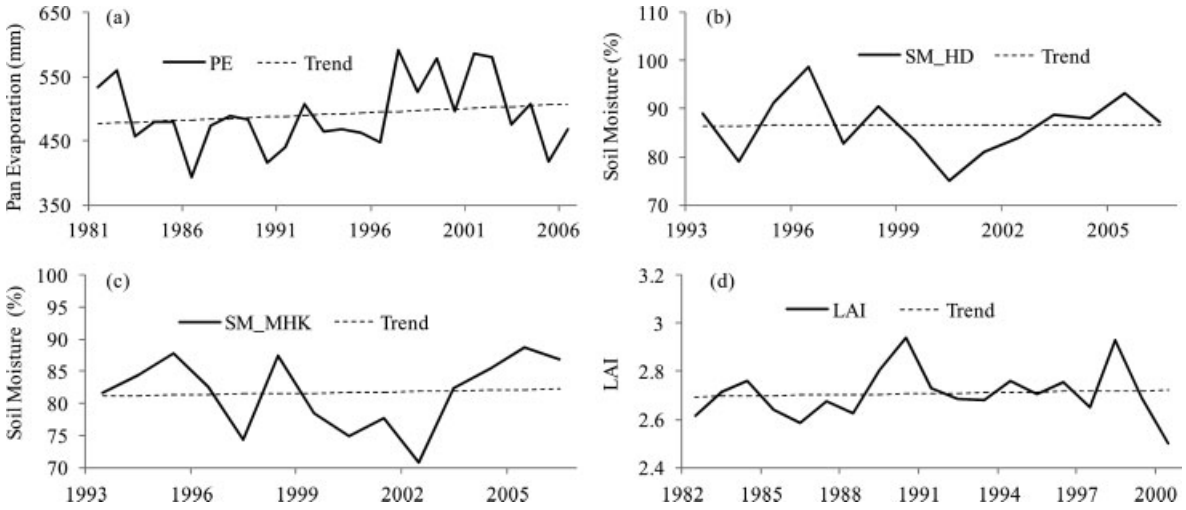

Figure 4. The changes in annual mean PE at the Huadian station (a) from 1981 to 2006, surface 10-cm SM at the Huadian (b) and Meihekou (c) stations from 1993 to 2006, and basin average LAI (d) from 1982 to 2000.

between 1957 and 2006. The SD and the DTR show similar variation trends during the study period. Liu *et al.* (2004b) noted that the SD may affect DTR through the imbalance effects on T_{max} and T_{min}. A detailed discussion is provided in the following section.

Figures 2(i) depicts the change in $R_{sw,d}$ from 1961 to 2006. $R_{sw,d}$ shows a decreasing trend with a magnitude equal to $-12.03\ \mathrm{W/m^2}$ per 50 years. Previous studies have shown that the decreasing trend ranges from $-10.5\ \mathrm{W/m^2}$ per 50 years to $22.5\ \mathrm{W/m^2}$ per 50 years during the period from 1961 to 2000 over China (Che *et al.*, 2005; Shi *et al.*, 2008; Tang *et al.*, 2011). The decline in $R_{sw,d}$ is also detected worldwide (e.g., Wild *et al.*, 2007). The similarity in the variations of $R_{sw,d}$ and DTR implies that $R_{sw,d}$ possibly influences DTR changes. In addition, T_{max} could decrease with a decline of $R_{sw,d}$ if other meteorological variables and the land surface characteristics keep unchanged. However, T_{max} displays a significant increasing trend from 1957 to 2006. Greenhouse gases, such as water vapour, carbon dioxide, and nitrous oxide, may affect T_{max} by changing the distribution of net radiation (Liu *et al.*, 2010). It has been reported that the radiative forcing generated by an increase in the concentration of greenhouse gases may be the main reason for global warming (IPCC, 2007). T_{max} may be affected by increasing greenhouse gas concentration. Thus, an increasing trend of the T_{max} is detected from 1957 to 2006 in this region.

Figure 4(a)–(d) depict the variation in PE from 1981 to 2006, in SM_HD and SM_MHK from 1993 to 2006, and in LAI from 1982 to 2000. All four of the variables show an increasing trend, although it is not significant. The correlations between these variables and the DTR are discussed in the following section.

3.2.2. *Correlative analysis*

Figure 5 shows the relationship between the normalized anomaly of annual DTR and the normalized anomalies of other variables over the USSR. These variables include SD, PE, SM_HD and SM_MHK, $R_{sw,d}$, precipitation and LAI. Figure 6(a) and (b) provide the spatial distribution of the correlation coefficient (R) between DTR and SD and between DTR and precipitation, respectively.

DTR is strongly correlated with SD (Figures 5(a) and 6(a)), with R equal to 0.8173. This relationship was also found in Northeast India (Jhajharia and Singh, 2011) and in lower-elevation sites in the Swiss Alps (Rebetez and Beniston, 1998). SD is directly related to $R_{sw,d}$. One of the factors that contributes to this phenomenon in this region is the unbalanced effect of $R_{sw,d}$ on T_{max} and T_{min}. Liu *et al.* (2004b) reported that $R_{sw,d}$ is closely related to DTR during the period from 1955 to 2000 in China. The effect of $R_{sw,d}$ is greater for daytime T_{max} than for night-time T_{min}. This results in a larger increase in T_{min} than in T_{max} and thus a lower DTR. In this region, the R between $R_{sw,d}$ and DTR is equal to 0.5089 (Figure 5(e)).

Figure 5(b) shows the R between the DTR and PE from 1981 to 2006. There is a high positive correlation between the DTR and PE, with R equal to 0.6701. The similarity between the variation in DTR and that in PE is consistent with previous reports (e.g. Peterson *et al.*, 1995; Roderick and Farquhar, 2002; Liu *et al.*, 2004a).

Figure 5(c) and (d) plot the correlation between DTR and SM_HD and between DTR and SM_MHK (top 10 cm of soil) during May and September from 1993 to 2006. The SM is negatively correlated with the DTR, with R equal to -0.5348 and -0.8167 for the Huadian station and the Meihekou station, respectively. Many studies (Dai *et al.*, 1999; Stone and Weaver, 2002) have noted that SM can decrease the DTR through evaporative cooling during the day, when the planetary boundary layer is unstable and the potential for evapotranspiration is high. The evaporative cooling effect on T_{max} is larger than on T_{min}, especially under dry conditions. Therefore, the DTR decreased with increased SM.

Figure 5(f) shows the R between precipitation and DTR from 1957 to 2006. Precipitation has an inhibiting

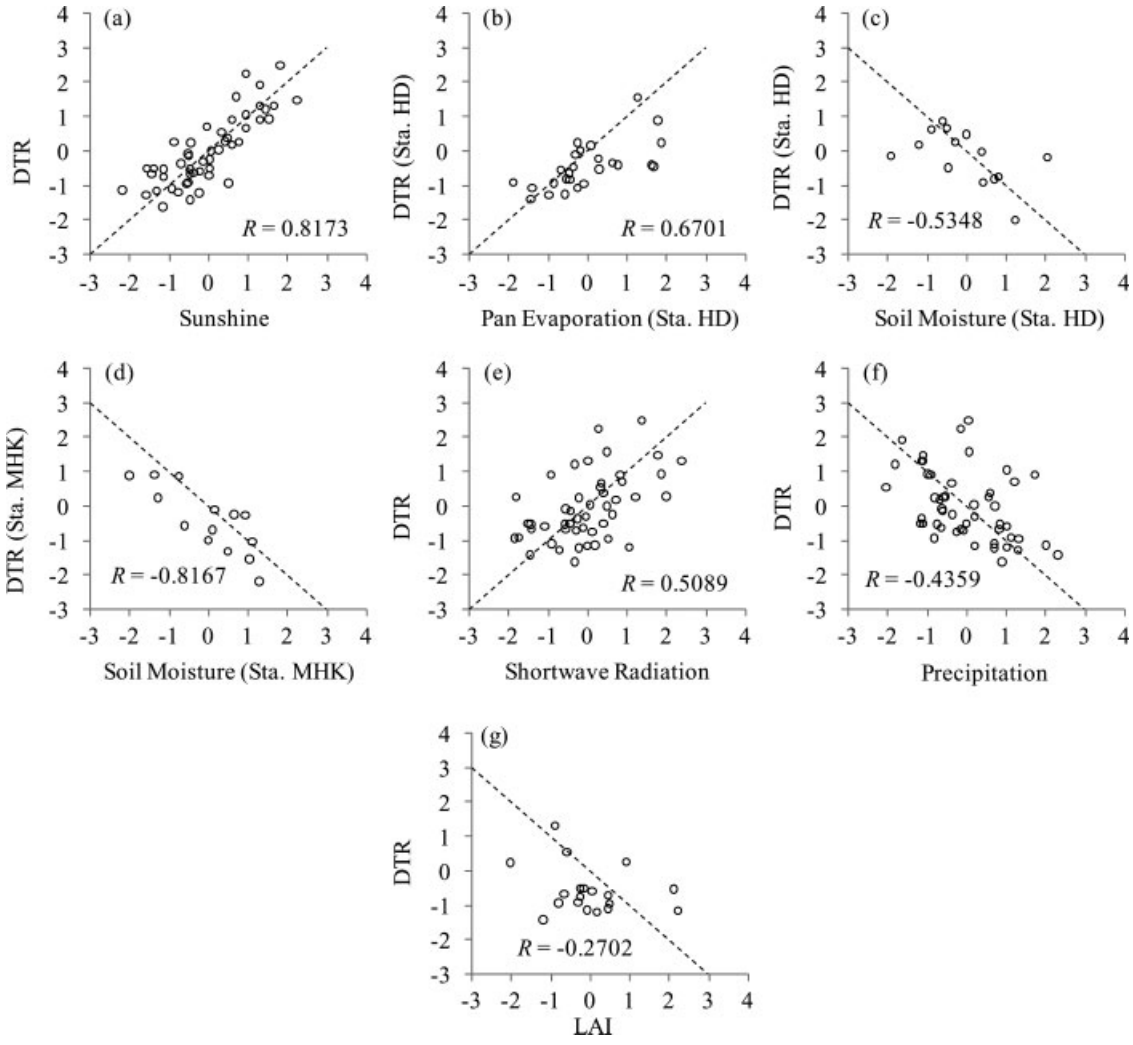

Figure 5. Comparison of normalized annual DTR with SD from 1957 to 2006 (a), PE from 1981 to 2006 (b), SM at the Huadian (c) and Meihekou (d) stations from 1993 to 2006, shortwave radiation from 1961 to 2006 (e), precipitation from 1957 to 2006 (f) and LAI from 1982 to 2000 (g).

effect on the DTR, with R equal to −0.4359. Many previous studies show that the evaporative cooling effect of precipitation may reduce the DTR (Dai *et al.*, 1999; Liu *et al.*, 2004b). The spatial distribution (Figure 6(b)) of R also indicates that precipitation and the DTR are negatively correlated over the USSR region.

Figure 5(g) indicates a negative correlation between the DTR and LAI, with R equal to −0.2702. This result is the opposite of that reported by Zhou *et al.* (2009). They found a strong positive correlation between the LAI and DTR over global land from 1950 to 2004. The result found in this study is probably caused by enhancing vegetation evaporative cooling effect through evapotranspiration. Increased evapotranspiration causes daytime cooling during the green season (Scheitlin and Dixon, 2010). Therefore, increases in LAI results in a decrease in the DTR.

The R between the DTR and CA and between the DTR and RH are 0.1581 and −0.0949 (not shown), respectively. These results indicate that the effects of CA and RH are small in this region.

3.2.3. *Summary*

The decrease in the DTR is mainly controlled by SD, PE and surface SM in the semiarid USSR. Other factors, such as precipitation and LAI, also affect the DTR. The R is low between the DTR and CA and between the DTR and RH. We found that SD is negatively correlated with SM, with R equal to −0.6442 and −0.6834 at the Huadian station and the Meihekou station, respectively. Thus, we suspect that SD may also affect the DTR through SM. Increased surface SM can increase latent heat release and slow down the increase in daytime T_{max} (Dai *et al.*, 1999). The DTR is then decreased as a result of the slower rate of increase in T_{max} relative to T_{min}. It is important to investigate the possible causes of the SD (or solar radiation) decrease because SD is the variable most closely correlated with the DTR.

3.3. The causes of SD change

Several factors can affect the variation in SD (or solar radiation), such as changes in cloud optical properties,

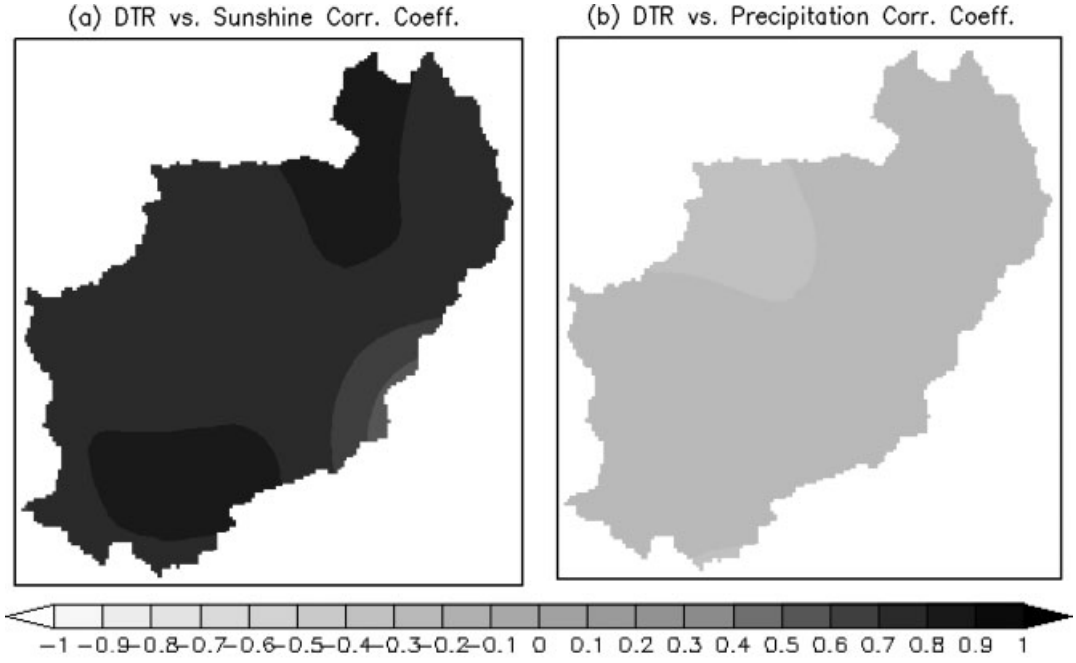

Figure 6. The correlation coefficients between the DTR and SD (a) and between the DTR and precipitation (b) from 1957 to 2006.

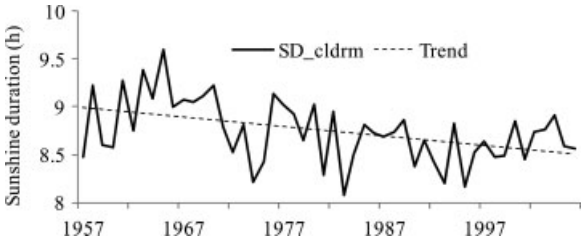

Figure 7. The annual mean SD and the linear trends on clear days (CA <0.1).

radiative active gases and the mass and optical properties of aerosols (Streets *et al.*, 2006; Qian *et al.*, 2007; Xu *et al.*, 2011). It has been suggested that clouds and aerosols are the most important of these factors (Xu *et al.*, 2011). Some studies relate a decrease in SD to a decline in CA (e.g. Wild *et al.*, 2005; Biggs *et al.*, 2007). However, cloud cover has been decreasing with solar irradiance in this region (see Figure 2(e) and (i)). Our analysis indicates that the SD trend is evident even when only clear-sky days are considered (Figure 7). Thus, aerosols are the primary contributors to this trend.

3.3.1. The role of aerosols on SD

Figure 8 plots the variation in the basin-averaged TOMS AI, the basin-averaged SD, and the ratio of diffuse to direct solar radiation (D_f/D_i). D_f and D_i constitute total $R_{sw,d}$ on a horizontal surface. The periods from 1979 to 1992 and from 1997 to 2005 (23 years total) are selected here because of the availability of the TOMS AI data.

Figure 8(a) shows the AI time series during the observation period. The annual mean AI varies from 0.22 (in 2005) to 0.97 (in 2001), with the average value equal to 0.50. The positive AI value indicates that the mineral dust, smoke and volcanic aerosols are the major aerosols in this basin. Zhang *et al.* (2011) also noted that a high mineral fraction exists in the northeast part of China.

Figure 8(b) depicts the mean annual SD under all-sky (SD) and aerosol-low sky (SD_Aero_rm) from 1979 to 2005. Aerosol-low sky is defined as a daily mean AI of <0.50 (23-year average AI). The average SD under an aerosol-low sky is 6.65 h, whereas it is 6.38 h under an all-sky condition during the 23-year period. This is reasonable because aerosols intercept sunshine (or solar radiation) on the way to the Earth's surface. Increased atmospheric aerosols resulting from industrial aerosols are known to reduce solar irradiance by reducing the amount of sunlight reaching the ground (Liu *et al.*, 2004b).

Figure 8(c) shows the variation in annual mean diffuse surface solar radiation (D_f) and the direct solar radiation (D_i) ratio (D_f/D_i) under all-sky and aerosol-low sky conditions from 1979 to 2005. The 23-year averages D_f/D_i under aerosol-low sky and under all-sky conditions are 0.85 and 0.91, respectively. Previous studies (e.g. Qian *et al.*, 2007; Xu *et al.*, 2011) noted that increasing of atmospheric aerosols can enhance scattering in the atmosphere, whereas they result in a decrease in atmospheric transparency. This mechanism likely explains the corresponding lower value of (D_f/D_i) under aerosol-low sky compared to the value under all-sky in this region.

3.3.2. Summary

In general, the SD was reduced by 0.27 h year^{-1} because of the aerosol effect. It should be noted that the threshold for AI was set to 0.50 because only 23 years of data are available for TOMS. The aerosol effect may not have been completely eliminated. This issue can be addressed

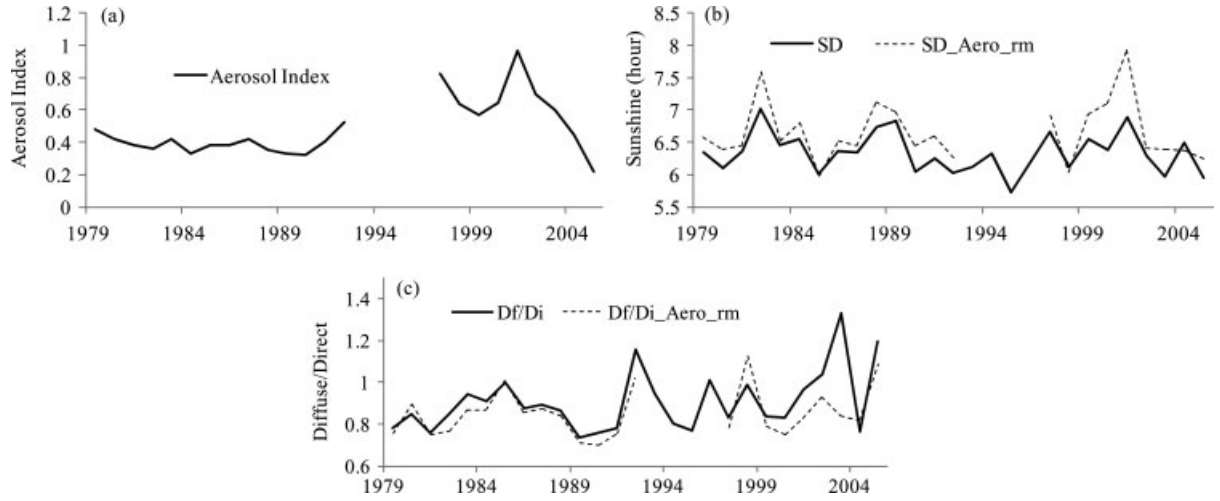

Figure 8. Time series of mean annual aerosol index (a), SD (b), and the ratio of diffuse to direct solar radiation (D_f/D_i) (c) from 1979 to 2005 in the USSR. The dashed lines (b and c) represent the aerosol-low values of SD and D_f/D_i by removing the aerosol effect.

in future studies if both aerosol data and SD (or solar radiation) data are available for a long-term period.

4. Conclusions

The DTR is an important variable for detecting climate change (Sun *et al.*, 2006; Makowski *et al.*, 2008). The decreasing trend in DTRs has been observed worldwide since the 1950s (Karl *et al.*, 1991; Karl *et al.*, 1993; Dai *et al.*, 1997; Easterling *et al.*, 1997; Dai *et al.*, 1999; IPCC, 2007), especially over arid and semiarid regions (Zhou *et al.*, 2008; Zhou *et al.*, 2009). However, the mechanisms of DTR variation remain somewhat ambiguous due to the complexity of the relevant climatology. In this study, the effects of climate elements (e.g. precipitation, SD), vegetation indicators (LAI) and anthropogenic factors (e.g. aerosols) over a semiarid region (northeast part of China) were examined using 50 years (1957–2006) of daily observation data. The main conclusions are described below.

First, the T_{max}, T_{min} and T_m increased, whereas the DTR decreased over all parts of the USSR, as indicated by temporal and spatial analyses of the period from 1957 to 2006. The rates of increase in T_{max} and T_{min} are 1.00 K per 50 years and 2.24 K per 50 years, respectively, whereas the rate of decrease in the DTR is −1.24 K per 50 years. The decrease in the DTR is mainly attributed to the higher rate of increase for T_{min} relative to T_{max}. This result is consistent with many previous studies (Karl *et al.*, 1991; Karl *et al.*, 1993; Dai *et al.*, 1997; Easterling *et al.*, 1997; Dai *et al.*, 1999; Liu *et al.*, 2004b).

Second, the causes of the DTR decrease were investigated by analysing the temporal trends and R of climatological and vegetation parameters. These parameters include CA, precipitation, RH, SD, $R_{sw,d}$, PE, SM and LAI. The results show that CA and RH appeared not to be the main cause of the decrease in DTR in this region. SD, PE and $R_{sw,d}$ have positive correlations with the DTR, whereas the SM, precipitation and LAI show negative correlations with the DTR.

SD has the most significant relationship with the DTR, with R equal to 0.8173. SD may affect the DTR in two ways. Through the unbalanced impact of $R_{sw,d}$ on T_{max} and T_{min}, the daytime T_{max} is more sensitive than the night-time T_{min} to $R_{sw,d}$. The decrease in $R_{sw,d}$ results in a relatively lower increase in T_{max} compared to the increase observed in T_{min}. The second possible influence comes from surface SM. Increasing SM can increase daytime latent heat release. An increase in daytime T_{max} is then slowed due to a cooling effect of evaporation (Dai *et al.*, 1999). Therefore, DTR decreases because T_{max} increases more slowly than T_{min}.

Precipitation and LAI reduces the DTR through evaporative cooling. Therefore, increases in precipitation and the LAI also result in a decrease in the DTR.

Third, the role of aerosols on solar radiation reduction was determined by analysing the TOMS AI from 1979 to 1992 and from 1997 to 2005. Mineral dust and smoke are the major aerosols in the study region. SD is reduced by 0.27 h year^{-1} as a result of decreasing atmospheric transparency induced by aerosols. Because aerosols can enhance scattering in the atmosphere, the ratio of annual mean diffuse surface solar radiation (D_f) and direct solar radiation (D_i) is higher under all-sky conditions than under aerosol-low sky conditions in this region.

In general, DTR variation is controlled by a number of factors. In addition to the meteorology and the anthropogenic factors analysed in this study, other factors (e.g. greenhouse gasses) may also affect DTR changes (IPCC, 2007). Further analysis regarding the causes of DTR variation is necessary. Given the importance of climate change (Piao *et al.*, 2010), further research is also encouraged to assess the impact of climate variation on the water and energy cycles in this region.

Acknowledgements

This study was supported by National Basic Research and Development Program of China (973, Grant No. 2013CB036401) and National Natural Science Foundation of China (Grant No. 51079014). The authors are deeply indebted to anonymous reviewers for their valuable comments and suggestions that greatly improve the quality of this manuscript.

References

Biggs TW, Scott CA, Rajagopalanc B, Turrald HN. 2007. Trends in solar radiation due to clouds and aerosols, southern India, 1952–1997. *International Journal of Climatology* **27**: 1505–1518. DOI: 10.1002/joc.1487

Campbell G, Vonder Haar T. 1997. Comparison of surface temperature minimum and maximum and satellite measured cloudiness and radiation budget. *Journal of Geophysical Research* **102**: D14. DOI: 10.1029/96JD02718

Che HZ, Shi GY, Zhang XY, Arimoto R, Zhao JQ, Xu L, Wang B, Chen ZH. 2005. Analysis of 40 years of solar radiation data from China, 1961–2000. *Geophysical Research Letters* **32**: L06803. DOI: 10.1029/2004GL022322

Dai A, Del Genio AD, Fung IY. 1997. Clouds, precipitation and temperature range. *Nature* **386**: 665–666. DOI: 10.1038/386665b0

Dai A, Trenberth KE, Karl TR. 1999. Effects of clouds, soil moisture, precipitation, and water vapor on diurnal temperature range. *Journal of Climate* **12**: 2451–2473.

Easterling DR, Horton B, Jones PD, Peterson TC, Karl TR, Parker DE, Salinger MJ, Razuvayev V, Plummer N, Jamason P, Folland CK. 1997. Maximum and minimum temperature trends for the globe. *Science* **277**: 364–367. DOI: 10.1126/science.277.5324.364

Fan ZX, Bräuning A, Thomas A, Li JB, Cao KF. 2011. Spatial and temporal temperature trends on the Yunnan Plateau (Southwest China) during 1961–2004. *International Journal of Climatology* **31**: 2078–2090. DOI: 10.1002/joc.2214

Feddema JJ, Oleson KW, Bonan GB, Mearns LO, Buja LE, Meehl GA, Washington WM. 2005. The importance of land-cover change in simulating future climates. *Science* **310**: 1674–1678. DOI: 10.1126/science.1118160

Herman JR, Bhartia PK, Torres O, Hsu C, Seftor C, Celarier E. 1997. Global distribution of UV-absorbing aerosols from Nimbus 7/TOMS data. *Journal of Geophysical Research* **102**: 16911–16922. DOI: 10.1029/96JD03680

Intergovernmental Panel on Climate Change. 2007. Chapter 2: Fourth Assessment Report (AR4). In *Climate Change 2007: The Physical Science Basis, Contribution of Working Group I to the Fourth Assessment Report of the Intergovernmental Panel on Climate Change*, Solomon S, Qin D, Manning M, Chen Z, Marquis M, Averyt KB, Tignor M, Miller HL (eds). Cambridge University Press: Cambridge, UK and New York, NY; 131–132.

Jhajharia D, Singh VP. 2011. Trends in temperature, diurnal temperature range and sunshine duration in Northeast India. *International Journal of Climatology* **31**: 1353–1367. DOI: 10.1002/joc.2164

Kaiser DP. 2000. Decreasing cloudiness over China: An updated analysis examining additional variables. *Geophysical Research Letters* **27**: 2193–2196. DOI: 10.1029/2000GL011358

Karl TR, Kukla G, Razuvayev VN, Changery MJ, Quayle RG, Heim RR Jr, Easterling DR, Fu CB. 1991. Global warming: evidence for asymmetric diurnal temperature change. *Geophysical Research Letters* **18**: 2253–2256. DOI: 10.1029/91GL02900

Karl TR, Jones PD, Knight RW, Kukla G, Plummer N, Razuvayev V, Gallo KP, Lindseay J, Charlson RJ, Peterson TC. 1993. Asymmetric trends of daily maximum and minimum temperature. *Bulletin of the American Meteorological Society* **74**: 1007–1023.

Lai LW, Cheng WL. 2010. Air temperature change due to human activities in Taiwan for the past century. *International Journal of Climatology* **30**: 432–444. DOI: 10.1002/joc.1898

Liu B, Xu M, Henderson M, Gong W. 2004a. A spatial analysis of pan evaporation trends in China, 1955–2000. *Journal of Geophysical Research* **109**: D15102. DOI: 10.1029/2004JD004511

Liu B, Xu M, Henderson M, Qi Y, Li Y. 2004b. Taking China's temperature: daily range, warming trends, and regional variations, 1955–2000. *Journal of Climate* **17**: 4453–4462. DOI: 10.1175/3230.1

Liu C, Liu X, Zhang H, Zeng Y. 2010. Change of the solar radiation and its causes in the Haihe River Basin and surrounding areas. *Journal of Geographical Sciences* **20**: 569–580. DOI: 10.1007/s11442-010-0569-z

Makowski K, Wild M, Ohmura A. 2008. Diurnal temperature range over Europe between 1950 and 2005. *Atmospheric Chemistry and Physics* **8**: 6483–6498. DOI: 10.5194/acp-8-6483-2008

Martínez MD, Serra C, Burgueño A, Lana X. 2010. Time trends of daily maximum and minimum temperatures in Catalonia (ne Spain) for the period 1975–2004. *International Journal of Climatology* **30**: 267–290. DOI: 10.1002/joc.1884

Myneni RB, Nemani RR, Running SW. 1997. Estimation of global leaf area index and absorbed par using radiative transfer models. *IEEE Transactions on Geoscience and Remote Sensing* **35**: 1380–1393. DOI: 10.1109/36.649788

Peterson TC, Golubev VS, Groisman PY. 1995. Evaporation losing its strength. *Nature* **377**: 687–688. DOI: 10.1038/377687b0

Piao S, Ciais P, Huang Y, Shen Z, Peng S, Li J, Zhou L, Liu H, Ma Y, Ding Y, Friedlingstein P, Liu C, Tan K, Yu Y, Zhang T, Fang J. 2010. The impacts of climate change on water resources and agriculture in China. *Nature* **467**: 43–51. DOI: 10.1038/nature09364

Przybylak R. 2000. Diurnal temperature range in the Arctic and its relation to hemispheric and Arctic circulation patterns. *International Journal of Climatology* **20**: 231–253.

Qian Y, Kaiser DP, Leung LR, Xu M. 2006. More frequent cloud-free sky and less surface solar radiation in China from 1955 to 2000. *Geophysical Research Letters* **33**: L01812. DOI: 10.1029/2005GL024586

Qian Y, Wang W, Leung LR, Kaiser DP. 2007. Variability of solar radiation under cloud-free skies in China: The role of aerosols. *Geophysical Research Letters* **34**: L12804. DOI: 10.1029/2006GL028800

Rebetez M, Beniston M. 1998. Changes in sunshine duration are correlated with changes in daily temperature range this century: An analysis of Swiss climatological data. *Geophysical Research Letters* **25**: 3611–3613. DOI: 10.1029/98GL02810

Roderick ML, Farquhar GD. 2002. The cause of decreased pan evaporation over the past 50 years. *Science* **298**: 1410–1411. DOI: 10.1126/science.1075390-a

Scheitlin KN, Dixon PG. 2010. Diurnal Temperature Range Variability due to Land Cover and Airmass Types in the Southeast. *Journal of Applied Meteorology and Climatology* **49**: 879–888. DOI: 10.1175/2009JAMC2322.1

Shi GY, Hayasaka T, Ohmura A, Chen ZH, Wang B, Zhao JQ, Che HZ, Xu L. 2008. Data quality assessment and the long-term trend of ground solar radiation in China. *Journal of Applied Meteorology and Climatology* **47**: 1006–1016. DOI: 10.1175/2007JAMC1493.1

Stone DA, Weaver AJ. 2002. Daily maximum and minimum temperature trends in a climate model. *Geophysical Research Letters* **29**: 1356. DOI: 10.1029/2001GL014556

Streets DG, Wu Y, Chin M. 2006. Two-decadal aerosol trends as a likely explanation of the global dimming/brightening transition. *Geophysical Research Letters* **33**: L15806. DOI: 10.1029/2006GL026471

Sun D, Pinker RT, Kafatos M. 2006. Diurnal temperature range over the United States: a satellite view. *Geophysical Research Letters* **33**: L05705. DOI: 10.1029/2005GL024780

Tang Q, Oki T, Kanae S, Hu H. 2007. A spatial analysis of hydroclimatic and vegetation condition trends in the Yellow River basin. *Hydrological Processes* **22**: 451–458. DOI: 10.1002/hyp.6624

Tang Q, Oki T, Kanae S, Hu H. 2008. Hydrological cycles change in the Yellow River Basin during the last half of the 20th century. *Journal of Climate* **21**: 1790–1806. DOI: 10.1175/2007JCLI1854.1

Tang WJ, Yang K, Qin J, Cheng CCK, He J. 2011. Solar radiation trend across China in recent decades: a revisit with quality-controlled data. *Atmospheric Chemistry and Physics* **11**: 393–406. DOI: 10.5194/acp-11-393-2011

Torres O, Bhartia PK, Herman JR, Ahmad Z, Gleason J. 1998. Derivation of aerosol properties from satellite measurements of backscattered ultraviolet radiation: Theoretical basis. *Journal of Geophysical Research* **103**: 17099–17110. DOI: 10.1029/98JD00900

Torres O, Bhartia PK, Herman JR, Sinyuk A, Ginoux P, Holben B. 2002. A long-term record of aerosol optical depth from TOMS observations and comparison to AERONET measurements. *Journal of the Atmospheric Sciences* **59**: 398–413.

Türkes M, Sümer UM, Kilic G. 1996. Observed changes in maximum and minimum temperatures in Turkey. *International Journal of Climatology* **16**: 463–477. DOI: 10.1002/(SICI)1097-0088(199604)16:4<463::AID-JOC13>3.0.CO;2-G

Wang A, Zeng X. 2011. Sensitivities of terrestrial water cycle simulations to the variations of precipitation and air temperature in China. *Journal of Geophysical Research* **116**: D02107. DOI: 10.1029/2010JD014659

Wang F, Wang L, Koike T, Zhou H, Yang K, Wang A, Li W. 2011. Evaluation and application of a fine-resolution global data set in a semiarid mesoscale river basin with a distributed biosphere hydrological model. *Journal of Geophysical Research* **116**: D21108. DOI: 10.1029/2011JD015990

Wang F, Wang L, Zhou H, Saavedra Valeriano OC, Koike T, Li W. 2012. Ensemble hydrological prediction based multi-objective reservoir real-time optimization during flood season in a semiarid basin with global numerical weather predictions. *Water Resources Research* **48**: W07520. DOI: 10.1029/2011WR011366

Wild M, Gilgen H, Roesch A, Ohmura A, Long CN, Dutton EG, Forgan B, Kallis A, Russak V, Tsvetkov A. 2005. From dimming to brightening: Decadal changes in solar radiation at Earth's surface. *Science* **308**: 847–850. DOI: 10.1126/science.1103215

Wild M, Ohmura A, Makowski K. 2007. Impact of global dimming and brightening on global warming. *Geophysical Research Letters* **34**: L04702. DOI: 10.1029/2006GL0280310

Xu J, Li C, Shi H, He Q, Pan L. 2011. Analysis on the impact of aerosol optical depth on surface solar radiation in the Shanghai megacity, China. *Atmospheric Chemistry and Physics* **11**: 3281–3289. DOI: 10.5194/acp-11-3281-2011

Zhang XY, Wang YQ, Niu T, Zhang XC, Gong SL, Zhang YM, Sun JY. 2011. Atmospheric aerosol compositions in China: spatial/temporal variability, chemical signature, regional haze distribution and comparisons with global aerosols. *Atmospheric Chemistry and Physics* **11**: 26571–26615. DOI: 10.5194/acpd-11-26571-2011

Zhou L, Dickinson RE, Tian Y, Vose R, Dai Y. 2007. Impact of vegetation removal and soil aridation on diurnal temperature range in a semiarid region: application to the Sahel. *Proceedings of the National Academy Sciences of the USA* **104**: 17937–17942. DOI: 10.1073/pnas.0700290104

Zhou L, Dickinson R, Dirmeyer P, Chen H, Dai Y, Tian Y. 2008. Asymmetric response of maximum and minimum temperatures to soil emissivity change over the Northern African Sahel in a GCM. *Geophysical Research Letters* **35**: L05402. DOI: 10.1029/2007GL032953

Zhou L, Dai A, Dai Y, Vose RS, Zou CZ, Tian Y, Chen H. 2009. Spatial dependence of diurnal temperature range trends on precipitation from 1950 to 2004. *Climate Dynamics* **32**: 429–440. DOI: 10.1007/s00382-008-0387-5

